Article

Suppressing Quadrature Error and Harmonics in Resolver Signals via Disturbance-Compensated PLL

Rui Wang * and Zhong Wu

School of Instrumentation and Optoelectronic Engineering, Beihang University, Beijing 100191, China
* Correspondence: wangrui2017@buaa.edu.cn

Abstract: The aim of this study was to obtain accurate angular positions and velocities from resolver signals; resolver-to-digital conversion (RDC) often adopts a phase-locked loop (PLL) as a demodulation algorithm. However, resolver signals often come with quadrature errors and harmonics, which lead to a severe reduction in PLL accuracy. The conventional PLL does not consider the impact of the quadrature error, and the bandwidth of the PLL is much larger than the fundamental frequency of resolver signals for pursuing a low dynamic error. These reasons render the retention of resolver harmonics in the demodulation results. In this paper, a disturbance-compensated PLL (DC-PLL) is proposed, which consists of a phase detector for suppressing quadrature error and harmonics (SQEH-PD) and a second-order observer. Firstly, since the quadrature error does not change with the angle velocity, the pre-estimated quadrature error is used in the SQEH-PD to compensate for the quadrature error in resolver signals. Secondly, although the frequency of the harmonics changes with the velocity, the amplitudes of the harmonics do not change. Therefore, the pre-estimated amplitudes of harmonics and estimated angular position are used in the SQEH-PD to compensate for the harmonics in resolver signals. Thirdly, a second-order observer is designed to estimate the angular position and velocity by regulating the phase detector error. Compared with the conventional PLL, the proposed DC-PLL has a stronger anti-disturbance ability against the quadrature error and harmonics by configuring the phase detector error and the estimated position error, which have a linear relation. Simulation and experimental results prove the effectiveness of the proposed method.

Keywords: resolver; PLL; phase detector; suppressing harmonics; quadrature error

1. Introduction

Resolvers are widely used in aviation, aerospace, and electric vehicle fields as angular position sensors for their advantages of high precision and strong anti-disturbance ability [1–3]. The outputs of resolvers are two orthogonal signals modulated by high-frequency excitation signals. To extract the accurate angular position and velocity from a resolver's signals, a high-precision RDC algorithm is usually adopted, which mainly includes detection and demodulation [4,5].

In the practical use of resolvers, there are many non-ideal factors in their signals, such as the quadrature error and harmonics [6]. The quadrature error refers to the fact that the phase difference between the two resolver signals is no longer 90 degrees [7]. Two major reasons are accounted for in the quadrature error: one is that the state windings are not installed orthogonally, and the other is that the number of winding turns is not ideal when rounding [8]. Harmonics refer to resolver signals containing harmonics of a rotor angular position. Harmonics are caused for two reasons: firstly, the inductance of winding is not ideal, and actual inductance induces harmonics, more or less [9]; secondly, the magnetic field of the resolver is distorted, which is usually caused by the non-ideal shape of the rotor [10]. Although quadrature error and harmonics have little effect on detection, they seriously reduce the accuracy of demodulation.

Demodulation algorithms can be divided into open-loop algorithms and closed-loop algorithms [11]. Although open-loop algorithms are simple and easy to implement, they often have poor anti-disturbance abilities. Commonly used inverse tangent algorithms [12] and the octant selection logic algorithm [13] have the problem of amplifying noise by differential operations [14]. Although the lookup table algorithm [15] and the pseudolinear signal algorithm [16] do not amplify noise, they have low demodulation accuracy and a poor anti-disturbance ability under the condition of limited processor resources.

Compared with open-loop algorithms, closed-loop algorithms have stronger anti-disturbance abilities, among which, a PLL is most commonly used for its high precision and strong anti-disturbance ability. A PLL consists of a phase detector (PD), a loop filter (LF), and a voltage-controlled oscillator (VCO) [17]. In [18], considering an unknown load torque and friction effects, a PLL is used to estimate the angle position, and a robust position backstepping tracking controller is designed to ensure the trajectory-tracking performance of the motor. In [19], a decoupled double synchronous reference frame-based PLL is proposed to suppress the amplitude imbalance in resolver signals. In [20], a composite PLL is proposed to suppress random disturbances, and the steady-state accuracy of the proposed composite PLL is greatly improved compared with the conventional PLL. However, the PLL has great defects in dealing with resolver signals containing the quadrature error and harmonics. To pursue a low dynamic error, the bandwidth of the PLL is often much larger than the fundamental frequency of resolver signals. Therefore, when there are harmonics in the resolver signals whose frequency is similar to that of the fundamental signal, the PLL fails to suppress harmonics. In addition, the conventional PLL does not consider the quadrature error in resolver signals, so it also fails to suppress the quadrature error.

In order to solve the problem of reduced demodulation precision by non-ideal factors of resolver signals, filtering and calibration methods are often used. In [21], low-pass filters are introduced to suppress harmonics. However, the frequency of harmonics is close to that of the fundamental signal. It is easy to damage the fundamental signal in the process of harmonics filtering, which introduces new errors in the RDC. In [22,23], two calibration algorithms are proposed to eliminate amplitude imbalances, DC offsets, and quadrature errors in resolver signals. However, the introduction of calibration increases the cost and reduces the reliability of the RDC. Moreover, the frequency of harmonics varies with the angular velocity, so it is difficult to suppress harmonics with calibration.

In this paper, a DC-PLL is proposed to suppress the quadrature error and harmonics in resolver signals. Firstly, since the quadrature error does not change with the angular velocity, the pre-estimated quadrature error can be used in SQEH-PD to compensate for the quadrature error in the resolver signals. Secondly, although the frequency of the harmonics changes with the velocity, the amplitudes of the harmonics do not change. Therefore, the estimated angular position is used to substitute the phase of the harmonics. The estimated angular position and pre-estimated harmonics amplitudes are used in the SQEH-PD to compensate for the harmonics in the resolver signals. Thirdly, the second-order observer estimates the angular position and the velocity by regulating the phase detector error from the SQEH-PD. For the resolver signals containing the quadrature error and harmonics, the proposed DC-PLL can improve the accuracy of the RDC significantly.

2. Effect of Non-Ideal Factors on RDC

2.1. RDC Principles

Figure 1 shows the principle of the software-based RDC. The resolver signals v_s^* and v_c^* are two orthogonal signals modulated with the excitation signal v_{ex}:

$$\begin{cases} v_s^* = v_1 \sin\theta \cos\omega_e t + \frac{\omega}{\omega_e} v_1 \cos\theta \sin\omega_e t \\ v_c^* = v_1 \cos\theta \cos\omega_e t - \frac{\omega}{\omega_e} v_1 \sin\theta \sin\omega_e t \end{cases} \tag{1}$$

where ω_e is the excitation frequency, which ranges from 1 to 10 kHz [24], and ω is the angular frequency of the rotor. Since ω_e is much bigger than ω, the second term of (1) can be regarded as zero [25]. The resolver signals can be expressed as [26]:

$$\begin{cases} v_s^* = v_1 \sin \theta \cos \omega_e t \\ v_c^* = v_1 \cos \theta \cos \omega_e t \end{cases} \tag{2}$$
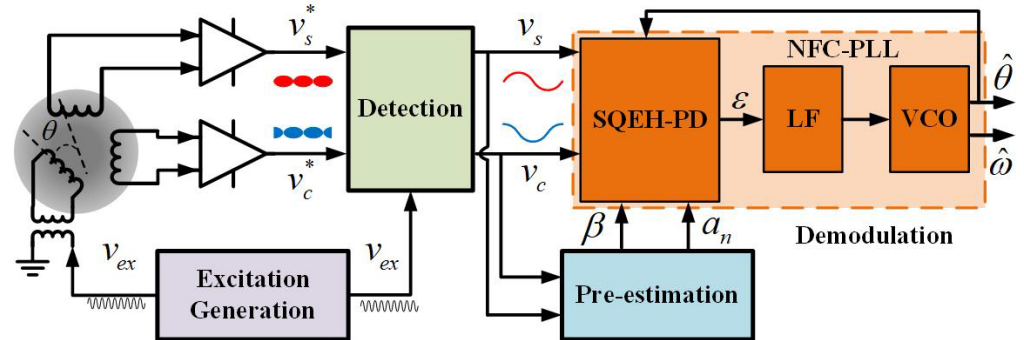

Figure 1. Schematic diagram of software-based RDC.

After detection, the pair envelope signals v_s and v_c were obtained as:

$$\begin{cases} v_s = sin\theta. \\ v_c = \cos \theta \end{cases} \tag{3}$$

When we inputted v_s and v_c into the demodulation, estimated position $\hat{\theta}$ and estimated velocity $\hat{\omega}$ were obtained. However, in the practical use of the resolver, the output signals were not the ideal form as shown in (3), and there were various non-ideal factors. Although some of them could be suppressed with calibration, they could not be eradicated completely, and the residual quadrature error and harmonics would seriously reduce the accuracy of the demodulation.

2.2. Analysis of Quadrature Error and Harmonics Effect on PLL

Using $\hat{\theta}$ denoted the estimated position from the PLL, and the phase detector error demodulated from the resolver signals shown in (3) could be expressed as:

$$\varepsilon = v_s \cos \hat{\theta} - v_c \sin \hat{\theta} \tag{4}$$

Substituting (3) into (4), the phase detector error was:

$$\varepsilon = \sin(\theta - \hat{\theta}) \approx \widetilde{\theta} \tag{5}$$

where θ is the actual position, $\widetilde{\theta} = \theta - \hat{\theta}$. Since $\widetilde{\theta}$ was very small, $\sin \widetilde{\theta} \approx \widetilde{\theta}$. The phase detector error reflects the difference between the actual and estimated positions. By regulating the phase detector error to equal 0, the estimated position and velocity could be obtained [27]. In the production of the resolver, the number of stator turns needed to be rounded so that the quadrature errors could be approximately equal to each order's harmonics to a certain extent [6]:

$$\begin{cases} v_s = \sin \theta + \sum_{n=2}^{\infty} a_n \sin n\theta \\ v_c = \cos(\theta - \beta) + \sum_{n=2}^{\infty} a_n \cos(n\theta - \beta) \end{cases} \tag{6}$$

where β expresses the value of the quadrature error, while a_n is the amplitude of harmonics. Substituting (6) into (4), the actual phase detector error was:

$$\varepsilon = \sin\theta \cos\hat{\theta} - \cos\theta \sin\hat{\theta} \cos\beta - \sin\theta \sin\hat{\theta} \sin\beta + \sum_{n=2}^{\infty} a_n \sin n\theta \cos\hat{\theta} - \sum_{n=2}^{\infty} a_n \cos n\theta \sin\hat{\theta} \cos\beta - \sum_{n=2}^{\infty} a_n \sin n\theta \sin\hat{\theta} \sin\beta \quad (7)$$

As (7) shows, when the quadrature error and harmonics existed in the resolver signals, the phase detector error contained many unexpected terms. It is impossible to make $\tilde{\theta}$ be zero by regulating ε to also be zero. That is the reason why the accuracy of the PLL reduced greatly when the resolver signals contained the quadrature error and harmonics.

3. Disturbance-Compensated PLL

In order to solve the problem of when the quadrature error and harmonics reduce the PLL accuracy, a DC-PLL was proposed, which was composed of the SQEH-PD and second-order observer. The schematic diagram is shown in Figure 2. The SQEH-PD was proposed to eliminate the quadrature error and harmonics in ε. Additionally, the second-order observer was used to estimate the angular position and velocity from ε. Strictly speaking, this paper studied the angle-tracking observer, which is a kind of PLL.
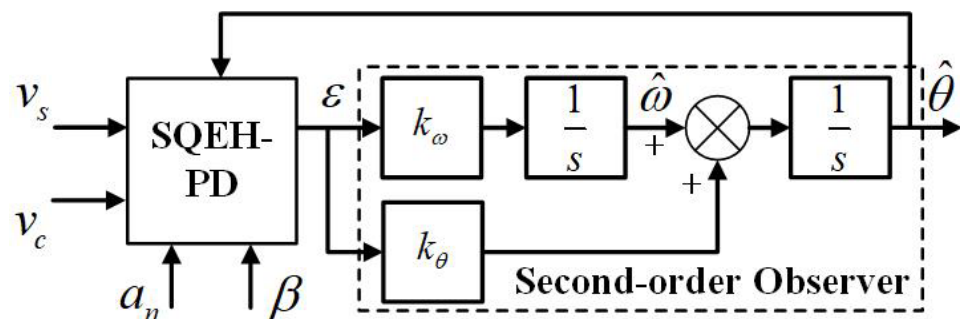

Figure 2. Schematic of the proposed DC-PLL.

3.1. Phase Detector for Suppressing Quadrature Error and Harmonics

The conventional PD simply feeds back the sinusoidal and cosinusoidal values of the estimated position, which makes the conventional PLL track not only the fundamental signal of the resolver, but also the non-ideal factor in resolver signals. Therefore, ε contains the quadrature error and the harmonics as shown in (7). Considering that the quadrature error and the amplitude of the harmonics would not change, the estimation method in [23] was adopted to obtain the value of the quadrature error, and the amplitudes of harmonics were obtained with the Fourier transform from the resolver signals.

As shown in Figure 3, the SQEH-PD could be expressed as:

$$\begin{cases} u_c = \cos\hat{\theta} + \tan\beta \sin\hat{\theta} + \sum_{n=2}^{\infty} a_n [\cos(n\hat{\theta}) + \tan\beta \sin(n\hat{\theta})] \\ u_s = \frac{1}{\cos\beta} [\sin\hat{\theta} + \sum_{n=2}^{\infty} a_n sin(n\hat{\theta})] \end{cases} \quad (8)$$

The phase detector error of SQEH-PD could be expressed as:

$$\varepsilon = v_s u_c - v_c u_s \quad (9)$$

By substituting (6) and (8) into (9), the phase detector error could be described as:

$$\varepsilon = \sin(\theta - \hat{\theta}) + \sum_{n=2}^{\infty} a_n \sin(n\theta - \hat{\theta}) + \sum_{n=2}^{\infty} a_n \sin(\theta - n\hat{\theta}) + \sum_{n=2}^{\infty} a_n \sin(n\theta) \sum_{n=2}^{\infty} a_n \cos(n\hat{\theta}) - \sum_{n=2}^{\infty} a_n \cos(n\theta) \sum_{n=2}^{\infty} a_n \sin(n\hat{\theta}) \quad (10)$$
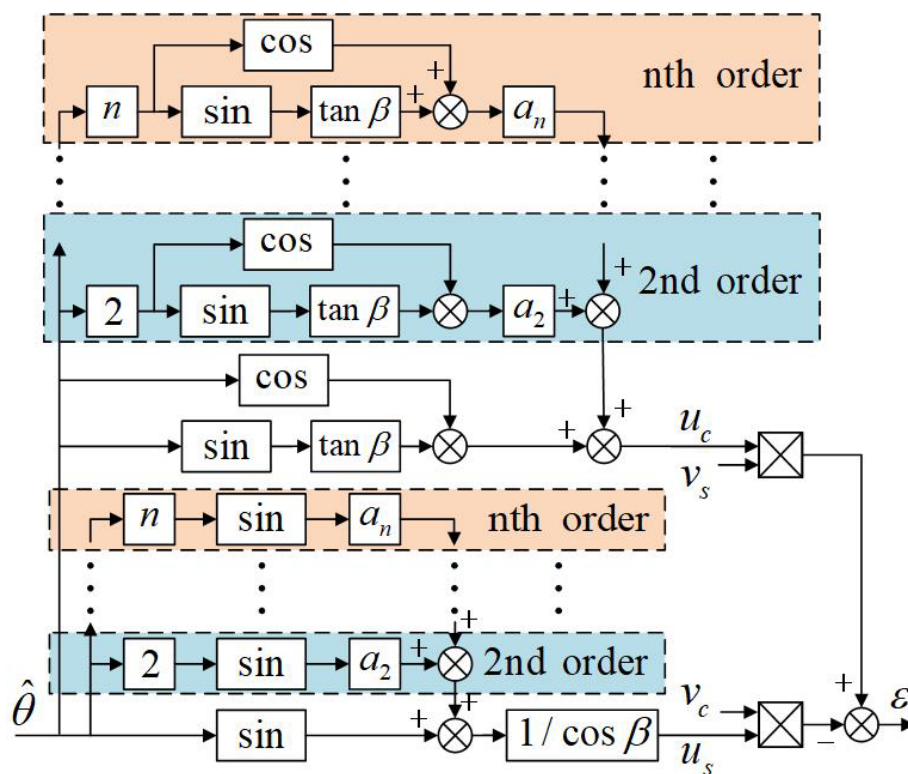
Figure 3. Schematic of proposed SQEH-PD.

In (10), ε had no correlation with the quadrature error, which indicated that the quadrature error was eliminated. ε could be divided into three parts: the terms without harmonics, the terms with harmonics, and the terms with the product of harmonics as:

$$\varepsilon_1 = \sum_{n=2}^{\infty} a_n \sin(n\theta - \hat{\theta}) + \sum_{n=2}^{\infty} a_n \sin(\theta - n\hat{\theta}) \tag{11}$$

$$\varepsilon_2 = \sum_{n=2}^{\infty} a_n \sin(n\theta) \sum_{n=2}^{\infty} a_n \cos(n\hat{\theta}) - \sum_{n=2}^{\infty} a_n \cos(n\theta) \sum_{n=2}^{\infty} a_n \sin(n\hat{\theta}) \tag{12}$$

The phase detector error could be rewritten as:

$$\varepsilon = \sin(\theta - \hat{\theta}) + \varepsilon_1 + \varepsilon_2 \tag{13}$$

where ε_1 could be simplified to:

$$\varepsilon_1 = \sum_{n=2}^{\infty} 2a_n \sin \frac{(n+1)(\theta - \hat{\theta})}{2} \cos \frac{(n-1)(\theta + \hat{\theta})}{2} \tag{14}$$

Considering the resolver manufacturing, the impact of the high-order harmonics was very low, so the high-order harmonics could be ignored [28]. Therefore, the following approximation could be used:

$$\begin{cases} \sin \frac{(n+1)(\theta - \hat{\theta})}{2} = \frac{(n+1)(\theta - \hat{\theta})}{2} \\ \cos \frac{(n-1)(\theta + \hat{\theta})}{2} = \cos(n-1)\theta \end{cases} \tag{15}$$

By substituting (15) into (14), ε_1 could be simplified as:

$$\varepsilon_1 = \sum_{n=2}^{\infty} a_n(n+1)(\theta - \hat{\theta})\cos(n-1)\theta \tag{16}$$

ε_2 could be simplified as:

$$\varepsilon_2 = \sum_{i=2}^{\infty} a_i^2 \sin[i(\theta - \hat{\theta})] + \sum_{\substack{j=3; \\ k=2; \\ j>k}}^{\infty} 2a_j a_k \sin\frac{(j+k)(\theta - \hat{\theta})}{2} \cos\frac{(j-k)(\theta + \hat{\theta})}{2} \tag{17}$$

In a similar way, substituting (15) into (17), ε_2 can be rewritten as:

$$\varepsilon_2 = \sum_{i=2}^{\infty} a_i^2 \sin[i(\theta - \hat{\theta})] + \sum_{\substack{j=3; \\ k=2; \\ j>k}}^{\infty} a_j a_k (j+k)(\theta - \hat{\theta})\cos(j-k)\theta \tag{18}$$

By substituting (16) and (18) into (13), the phase detector error can be expressed as:

$$\varepsilon = \sin\widetilde{\theta} + \sum_{n=2}^{\infty} a_n(n+1)\widetilde{\theta}\cos(n-1)\theta + \sum_{i=2}^{\infty} a_i^2 \sin i\widetilde{\theta} + \sum_{\substack{j=3; \\ k=2; \\ j>k}}^{\infty} a_j a_k (j+k)\widetilde{\theta}\cos(j-k)\theta \tag{19}$$

When $\hat{\theta}$ was close to θ, $\widetilde{\theta}$ could be considered very small, so (19) could be simplified to:

$$\varepsilon = \widetilde{\theta}[1 + \sum_{n=2}^{\infty} a_n(n+1)\cos(n-1)\theta + \sum_{i=2}^{\infty} a_i^2 i + \sum_{\substack{j=3; \\ k=2; \\ j>k}}^{\infty} a_j a_k (j+k)\cos(j-k)\theta] \tag{20}$$

In (20), ε and $\widetilde{\theta}$ had a linear relationship, so $\widetilde{\theta}$ could be actualized to be zero by regulating ε to be zero. Therefore, the proposed SQEH-PD could improve the accuracy of the PLL in the presence of harmonics and the quadrature error.

3.2. Second-Order Observer

By using the phase detector error ε from the SQEH-PD, a second-order observer could be designed to estimate the angular position $\hat{\theta}$ and velocity $\hat{\omega}$. As shown in Figure 2, the error transfer function of the angular position and velocity were expressed as:

$$E_\theta(s) = \frac{\widetilde{\theta}(s)}{\theta(s)} = \frac{s^2}{s^2 + k_\theta s + k_\omega} \tag{21}$$

$$E_\omega(s) = \frac{\hat{\omega}(s)}{\omega(s)} = \frac{s^2 + k_\theta s}{s^2 + k_\theta s + k_\omega} \tag{22}$$

where $\widetilde{\omega} = \omega - \hat{\omega}$. According to (21) and (23), the steady-state error of the angular position and velocity could be expressed as:

$$e_\theta(\infty) = \lim_{s \to 0} s E_\theta(s)\theta(s) \tag{23}$$

$$e_\omega(\infty) = \lim_{s \to 0} s E_\omega(s)\omega(s) \tag{24}$$

In the fixed-velocity conditions,$\omega = A$ was assumed. The Laplace transforms of the angular position and velocity were $\theta(s) = A/s^2$,$\omega(s) = A/s$, and when substituting them into (23) and (24), both $e_\theta(\infty)$ and $e_\omega(\infty)$ were zero. In the fixed-acceleration conditions, we assumed that $\omega = Bt$. The Laplace transforms of the angular position and velocity were $\theta(s) = B/s^3$, $\omega(s) = B/s^2$, and when substituting them into (23) and (24), $e_\theta(\infty) = B/k_\omega$ and $e_\omega(\infty) = Bk_\theta/k_\omega$. Obviously, the proposed second-order observer could give an accurate estimation of the angular position and velocity without steady-state errors in the fixed-velocity conditions, and with constant deviations in fixed-acceleration conditions.

4. Simulation and Experimental Results

4.1. Simulation Results

In order to verify the effectiveness of the proposed DC-PLL, a simulation was conducted in the MATLAB/Simulink platform. The pair envelopes of resolver signals were simulated directly with certain harmonics and the quadrature error as: 1 for the fundamental signal, 0.09% for the 3rd harmonic, 0.11% for the 5th harmonic, 0.15% for the 11th harmonic, 0.13% for the 13th harmonic, and 0.3° for the quadrature error. Considering that the resolver is often used as an angular position sensor of servo systems, three typical working conditions were selected: constant velocity, constant acceleration, and sinusoidal velocity. For ensuring the fairness of the comparison, the PLL parameters were chosen as $k_\theta = 888$, $k_\omega = 394,000$.

4.1.1. Case 1: Constant Velocity ($\omega = 360^\circ/s$)

Figure 4 shows the resolver signals. Figure 5 shows the spectrum of the resolver signals. It can be seen from Figure 5 that there were 3rd, 5th, 11th, and 13th harmonics in the resolver signals, which seriously reduced the demodulation accuracy.
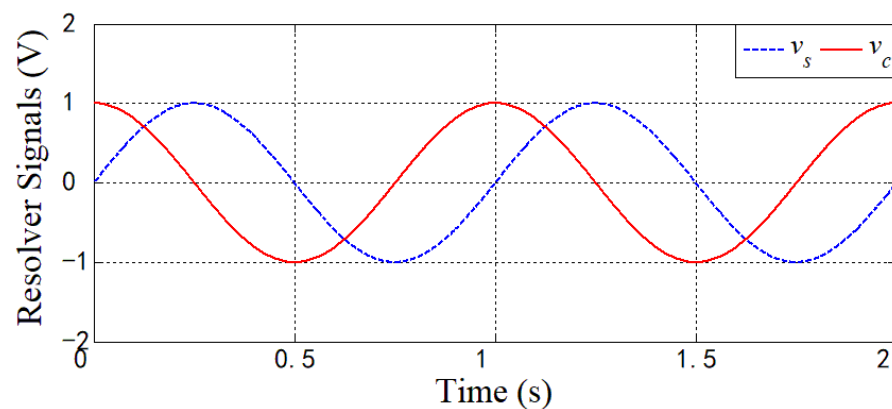

Figure 4. Resolver signals at fixed speed in simulation.

The conventional PLL and the proposed DC-PLL were used to demodulate the resolver signals. When the DC-PLL was adopted, it can be seen from Figure 6 that the phase detector error was basically zero, and the spectrum of the phase detector error did not contain any harmonics. In Figure 7, when the PLL was adopted, the harmonics in the resolver signals led to a large number of harmonics in the phase detector error, where the 2nd, 4th, 10th, and 12th harmonics were dominant.

Three methods were used to demodulate the resolver signals: the conventional PLL (PLL), the DC-PLL only for the quadrature error compensation (Compensate β), and the DC-PLL for the quadrature error and harmonics compensation (DC-PLL).

As shown in Figure 8a, due to the existence of the quadrature error, the position error was asymmetric about the *x*-axis when the PLL was adopted. However, when using the proposed DC-PLL for compensating the quadrature error, the asymmetric part of the position error was eliminated. Furthermore, when using the DC-PLL for compensating the quadrature error and the harmonics, the position error was greatly reduced, and the

disturbance of the quadrature error and the harmonics was completely eliminated. As shown in Figure 8b, the influence of the quadrature error on the velocity estimation was not as great as its influence on the position estimation. When using the DC-PLL to compensate for the harmonics disturbance, the velocity error was greatly reduced.
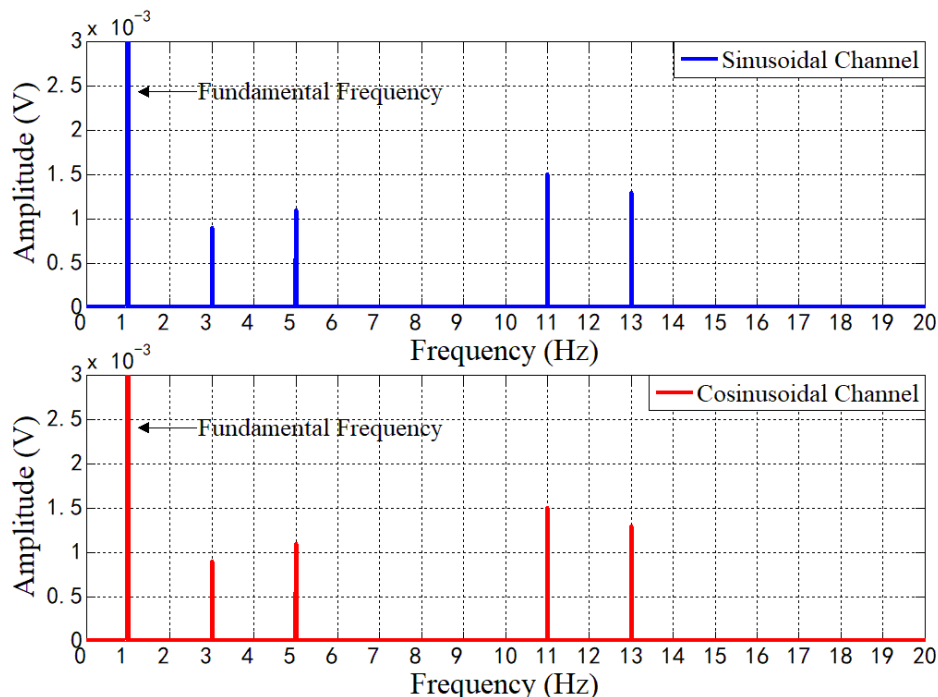

Figure 5. Spectrum of resolver signals at fixed speed in simulation.
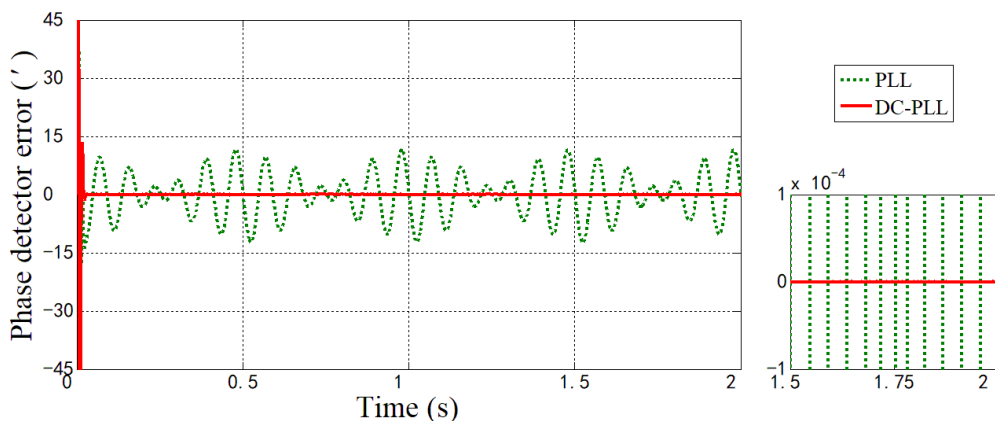

Figure 6. Phase detector error at fixed speed.

In order to show the performance of the proposed DC-PLL more clearly, the average (AVG) and the standard deviation (STD) were calculated under three working conditions. Table 1 shows the statistics of the position estimation error. Table 2 shows the statistics of the velocity estimation error. It is clear that the STD of the position estimation error and velocity estimation error with the DC-PLL were reduced by 99.9% and 99.9% compared with the PLL. In Table 1, the AVG of the DC-PLL was smaller than that of the PLL, which indicated that the DC-PLL had better performance on quadrature error suppression.
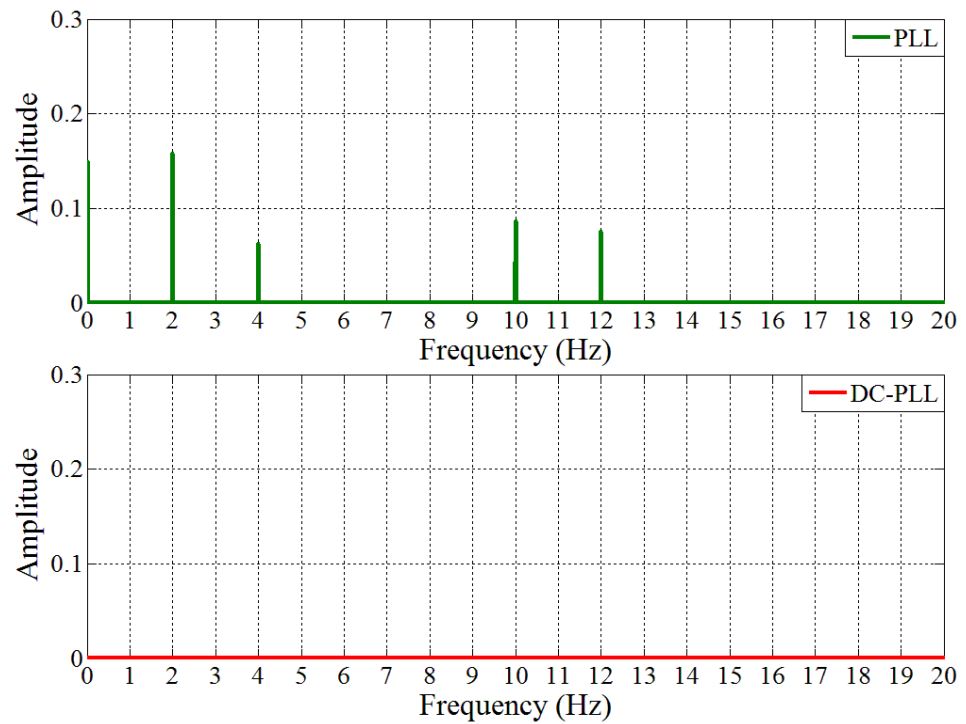
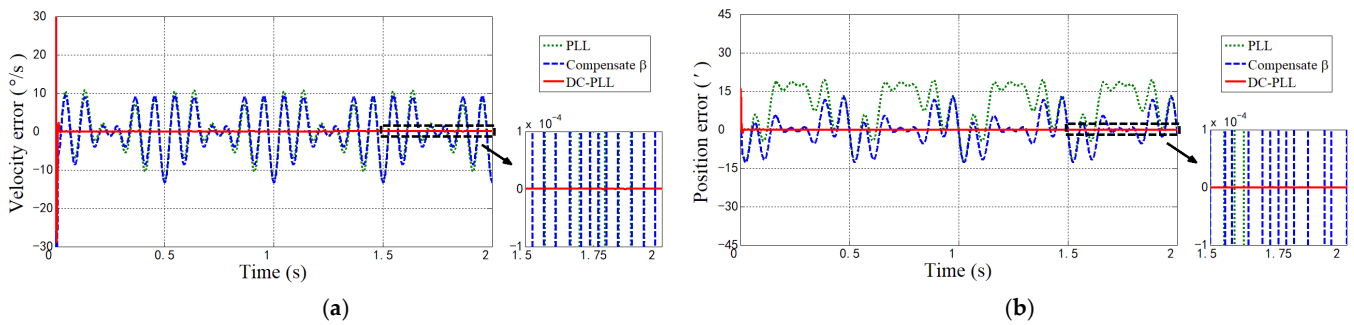**Figure 7.** Spectrum of phase detector error at fixed speed.

Figure 8. Demodulation errors at fixed speed in simulation. (**a**) Position estimation error; (**b**) velocity estimation error.

Table 1. The statistics of position estimation error ($\widetilde{\theta}(')$).

Cases		Case 1	Case 2	Case 3
PLL	AVG	9.008	9.104	9.747
	STD	8.747	9.012	8.391
Compensate β	AVG	2.009×10^{-5}	0.071	0.176
	STD	5.996	6.392	5.847
DC-PLL	AVG	3.811×10^{-12}	0.036	4.260×10^{-5}
	STD	4.721×10^{-11}	7.468×10^{-4}	0.1599

Table 2. The statistics of velocity estimation error ($\widetilde{\omega}(^\circ/s)$).

Cases		Case 1	Case 2	Case 3
PLL	AVG	2.211×10^{-7}	0.412	7.278×10^{-12}
	STD	5.819	17.814	6.443
Compensate β	AVG	2.195×10^{-7}	0.390	5.939×10^{-12}
	STD	5.664	17.350	6.323
DC-PLL	AVG	2.586×10^{-10}	0.379	1.288×10^{-12}
	STD	5.387×10^{-10}	0.002	1.733

4.1.2. Case 2: Constant Acceleration ($\omega = 180t \ ^\circ/s$)

In the case of constant acceleration, the influence of the quadrature error on the position estimation was obvious. As Figure 9a shows, when the PLL was used, the position error was asymmetric about the time-axis. This was because the quadrature error caused the phase detection error and position error to no longer have a linear relation. However, the proposed DC-PLL caused the phase detection error and position error to have a linear relation, so as to eliminate the influence of the quadrature error on the phase detection error. In Figure 9a, the position error of the DC-PLL was much smaller than that of the DC-PLL, only suppressing the quadrature error, which indicated that the proposed DC-PLL had a good ability of harmonics suppression.
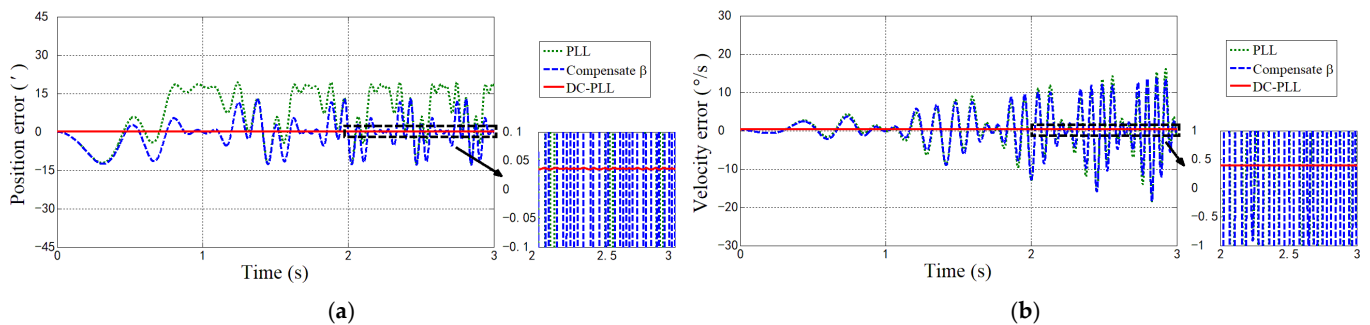

Figure 9. Demodulation errors at fixed acceleration in simulation. (**a**) Position estimation error; (**b**) velocity estimation error.

With the increase in velocity, the influence of the harmonics on velocity estimation became more and more serious. As Figure 9b shows, when the PLL was adopted, the velocity error became larger and larger. That was because the harmonics affected the position estimation through differential operations. Although the content of the harmonics was unchanged, the velocity error would become larger and larger with the increase in velocity. When the DC-PLL was adopted, the fluctuation in the velocity error was basically zero because of its good harmonics suppression.

As can be seen in Table 1, the AVG of the DC-PLL was reduced by 99.6% compared with PLL. It was clear that the proposed DC-PLL suppressed the quadrature error completely. In Tables 1 and 2, the STD of the position estimation error and velocity estimation error with the DC-PLL were reduced by 99.9% and 99.9%, respectively, compared with the PLL.

4.1.3. Case 3: Sinusoidal Velocity ($\omega = 720 + 90\sin(90t) \ ^\circ/s$)

In Figure 10a, when the DC-PLL was used to compensate for the quadrature error, the amplitude of the position error was symmetric about the x-axis, and the position error was greatly reduced. Because of the superior suppression on the quadrature error, the AVG of the DC-PLL was reduced by 99.9% compared with the PLL in Table 1. It can be seen from Figure 10b that the velocity error changed periodically. When the DC-PLL was adopted, the harmonics were well suppressed, so that the velocity error was the smallest among the three lines. From Tables 1 and 2, it could be seen that the STD of the position

estimation error and velocity estimation error with DC-PLL were reduced by 98.1% and 73.1% compared with the PLL.
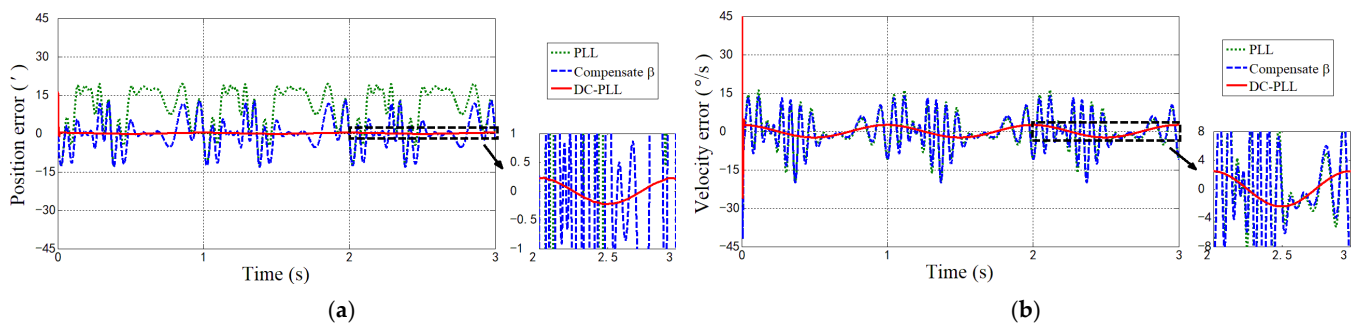

Figure 10. Demodulation errors at sinusoidal speed in simulation. (**a**) Position estimation error; (**b**) velocity estimation error.

4.2. Experiment Results

In order to verify the effectiveness of the proposed method, an experimental platform was used. As shown in Figure 11, the experimental platform was mainly composed of a permanent magnet synchronous motor (PMSM) with a resolver, a drive board, a power supply, and a PC. The parameters of the PMSM and the resolver are shown in Table 3. In the drive board, the resolver signals were, firstly, inputted into the AD7606 for envelope sampling, and then, the envelope signals were inputted into the DSP for calibrating the amplitude imbalance and the DC offset with the calibration method proposed in [1]; finally, the calibrated envelope signals were inputted into the PLL proposed in this paper to estimate the angular position and angular velocity. The estimated angular position was used to generate a reversing current, and the estimated angular velocity was used to control the motor running at a constant speed of $360°/s$. The power supply was responsible for providing a stable voltage to the drive board. The PC was responsible for receiving the demodulation results from the drive board. The quadrature error and the harmonics amplitudes were obtained with the calibration method in [23].
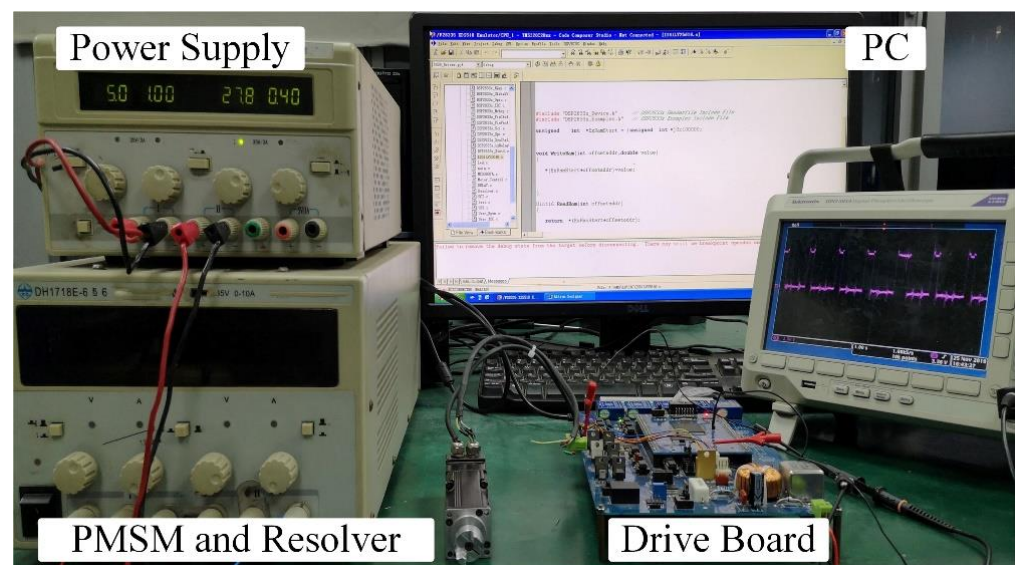

Figure 11. Experimental platform.

Table 3. Parameters of PMSM and resolver.

PMSM		Resolver	
Pole pairs	2	Pole pairs	1
Rated speed	3000 r/min	Excitation frequency	10 kHz
Torque constant	0.15 Nm/A	Electrical error	10′
Phase resistance	8 Ω	Input impedance	95 ± 14 Ω
Phase inductance	10 mH	Quadrature error	0.3°

The resolver signals after detection are shown in Figure 12. Figure 13 shows the spectrum of the resolver signals, and the harmonics were mainly 2nd, 3rd, 5th, 11th, and 13th. However, these harmonics were not only caused by the resolver itself, but the cogging effect of the motor also affected the harmonics content.
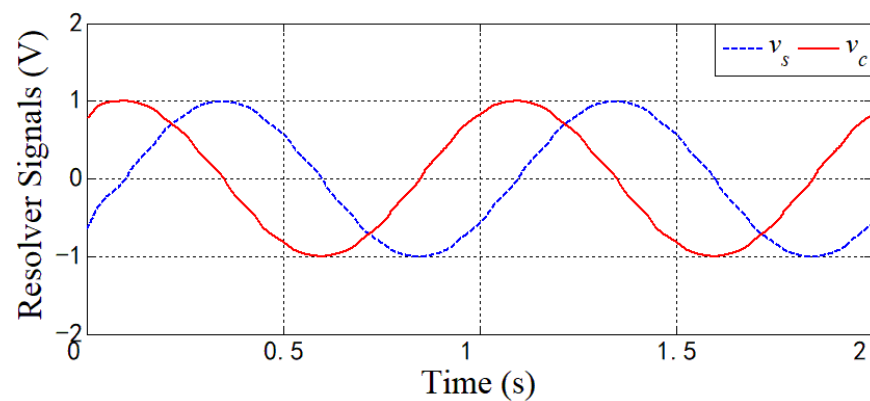
Figure 12. Resolver signals at fixed speed in experiment.
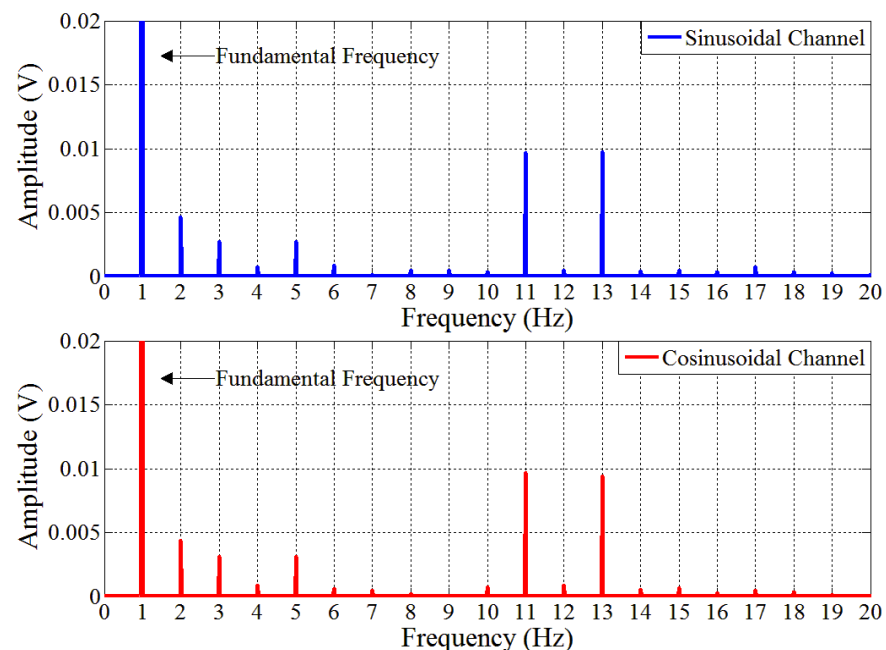
Figure 13. Spectrum of resolver signals at fixed speed in experiment.

Different from the simulation, the true angular position and angular velocity could not be obtained in the experiment. Therefore, to compare the estimation accuracy of the DC-PLL and the PLL, the phase detector error was used to measure the accuracy of the position estimation instead of the position error, and the estimated velocity was used to measure the accuracy of the velocity estimation instead of the velocity error.

It can be seen from Figure 14 that there were a lot of harmonics in the phase detector error when using the PLL, which greatly decreased the accuracy of the position estimation. However, when the DC-PLL was used, the harmonics in the phase detector error were obviously suppressed. In Figure 15, the fluctuation of the DC-PLL was the smallest among the three curves, which indicated that the DC-PLL had good performance on harmonics suppression.
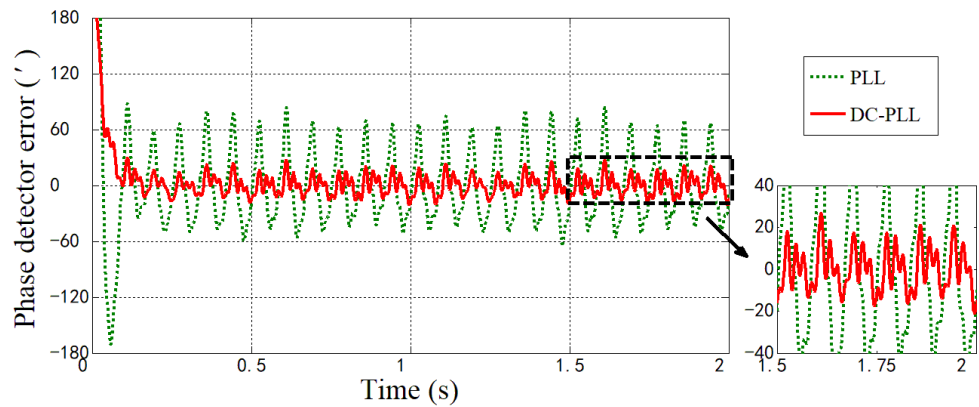

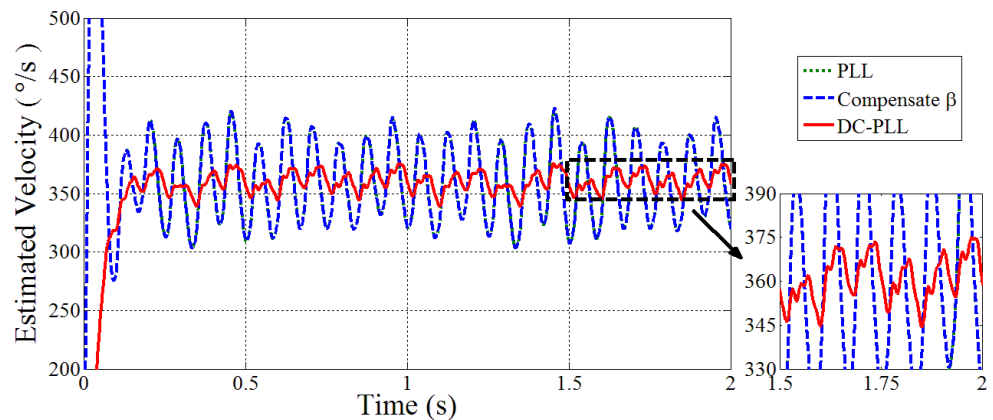**Figure 14.** Phase detector error at fixed speed in experiment.

Figure 15. Velocity estimation at fixed speed in experiment.

In Table 4, when comparing the phase detector error, the AVG of the DC-PLL was nearly an order of magnitude smaller than that of the PLL, which indicated that the DC-PLL had a better suppression ability on the quadrature error. Comparing the estimated velocity, the AVG of the DC-PLL was closer to $360°/s$ than that of the PLL. Moreover, the STD of the phase detector error and estimated velocity with the DC-PLL was reduced by 72.0% and 74.5% compared with the PLL.

Table 4. The statistics of experiment demodulation results.

Cases		$\boldsymbol{\varepsilon(')}$	$\boldsymbol{\hat{\omega}(°/s)}$
PLL	AVG	2.482×10^{-4}	359.999504
	STD	37.335	32.6144
DC-PLL	AVG	3.620×10^{-5}	359.999721
	STD	10.443	8.333

5. Conclusions

In this paper, a disturbance-compensated PLL was proposed, in which the phase detector for suppressing the quadrature error and harmonics was the main component. In the proposed phase detector, the estimated angular position was used to substitute the

phase of the harmonics, and the harmonics of the resolver signals were compensated with the estimated angular position and the pre-estimated harmonics amplitudes. Additionally, the quadrature error in the resolver signals was compensated in the proposed phase detector by using the quadrature error estimated in advance. Compared with the traditional PLL, the proposed method could suppress the quadrature error and harmonics better by making the phase detector error and position error have a linear relation, and improving the anti-disturbance ability without changing the bandwidth. Simulation and experimental results showed that the proposed method had good performance on the quadrature error and harmonics suppression.

Author Contributions: Z.W. and R.W. conceived the research; R.W. performed the experiments and wrote the paper; Z.W. guided the experiments and contributed to the revising of the paper; R.W. provided the hardware and software support and data analysis. All authors have read and agreed to the published version of the manuscript.

Institutional Review Board Statement: Not applicable.

Informed Consent Statement: Not applicable.

Data Availability Statement: Not applicable.

Conflicts of Interest: The authors declare no conflict of interest.

References

1. Sabatini, V.; Benedetto, M.D.; Lidozzi, A. Synchronous adaptive resolver-to-digital converter for FPGA-based high-performance control loops. *IEEE Trans. Instrum. Meas.* **2019**, *68*, 3972–3982. [CrossRef]
2. Yepes, A.G.; Lopez, O.; Gonzalez-Prieto, I.; Duran, M.J.; Doval-Gandoy, J. A Comprehensive survey on fault tolerance in multiphase AC drives, part 1: General overview considering multiple fault types. *Machines* **2022**, *10*, 208. [CrossRef]
3. Saneie, H.; Nasiri-Gheidari, Z.; Tootoonchian, F. Structural design and analysis of a high reliability multi-turn wound-rotor resolver for electric vehicle. *IEEE Trans. Veh. Technol.* **2020**, *69*, 4992–4999. [CrossRef]
4. Estrabis, T.; Gentil, G.; Rordero, R. Development of a resolver-to-digital converter based on second-order difference generalized predictive control. *Energies* **2012**, *14*, 459. [CrossRef]
5. Khaburi, D.A. Software-based resolver-to-digital converter for DSP-based drives using an improved angle-tracking observer. *IEEE Trans. Instrum. Meas.* **2012**, *61*, 922–929. [CrossRef]
6. Hanselman, D.C. Resolver signal requirements for high accuracy resolver-to-digital conversion. *IEEE Trans. Ind. Electron.* **1990**, *37*, 556–561. [CrossRef]
7. Kaul, S.K.; Tickoo, A.K.; Koul, R.; Kumar, N. Improving the accuracy of low-cost resolver-based encoders using harmonic analysis. *Nucl. Instrum. Methods Phys. Res. A* **2008**, *586*, 345–355. [CrossRef]
8. Hanselman, D.C. Techniques for improving resolver-to-digital conversion accuracy. *IEEE Trans. Ind. Electron.* **1991**, *38*, 501–504. [CrossRef]
9. Robinson, R.B. Inductance coefficients of rotating machines expressed in terms of winding space harmonic. *Proc. Inst. Electr. Eng.* **1964**, *111*, 769–774. [CrossRef]
10. Ge, X.; Zhu, Z.Q. A novel design of rotor contour for variable reluctance resolver by injecting auxiliary air-gap permeance harmonics. *IEEE Trans. Energy Convers.* **2016**, *31*, 345–353. [CrossRef]
11. Wang, F.; Shi, T.; Yan, Y.; Wang, Z.; Xia, C. Resolver-to-digital conversion based on acceleration-compensated angle tracking observer. *IEEE Trans. Instrum. Meas.* **2019**, *68*, 3494–3502. [CrossRef]
12. Bahari, M.; Davoodi, A.; Saneie, H.; Tootoonchian, F.; Nasiri-Gheidari, Z. A new variable reluctance PM-resolver. *IEEE Sens. J.* **2020**, *20*, 135–142. [CrossRef]
13. Sarma, S.; Agrawal, V.K.; Udupa, S. Software-based resolver-to-digital conversion using a DSP. *IEEE Trans. Ind. Electron.* **2008**, *55*, 371–379. [CrossRef]
14. Hou, C.; Chiang, Y.; Lo, C. DSP-based resolver-to-digital conversion system designed in time domain. *IET Power Electron.* **2014**, *7*, 2227–2232. [CrossRef]
15. Kamf, T.; Abrahamsson, J. Self-sensing electromagnets for robotic tooling systems: Combining sensor and actuator. *Machines* **2016**, *4*, 16. [CrossRef]
16. Wang, S.; Kang, J.; Degano, M.; Buticchi, G. A Resolver-to-digital conversion method based on third-order rational fraction polynomial approximation for PMSM control. *IEEE Trans. Ind. Electron.* **2019**, *66*, 6383–6392. [CrossRef]
17. Herrejón-Pintor, G.A.; Melgoza-Vázquez, E.; Chávez, J.D.J. A modified SOGI-PLL with adjustable refiltering for improved stability and reduced response time. *Energies* **2022**, *15*, 4253. [CrossRef]

18. Linares-Flores, J.; García-Rodríguez, C.; Sira-Ramírez, H.; Ramírez-Cárdenas, O.D. Robust backstepping tracking controller for low-speed PMSM positioning system: Design, analysis, and implementation. *IEEE Trans. Ind. Inform.* **2015**, *11*, 1130–1141. [CrossRef]

19. Bergas-Jané, J.; Ferrater-Simón, C.; Gross, G.; Ramírez-Pisco, R.; Galceran-Arellano, S.; Rull-Duran, J. High-accuracy all-digital resolver-to-digital conversion. *IEEE Trans. Ind. Electron.* **2012**, *59*, 326–333. [CrossRef]

20. Zhang, J.; Wu, Z. Composite state observer for resolver-to-digital conversion. *Meas. Sci. Technol.* **2017**, *28*, 065103. [CrossRef]

21. Sivappagari, C.M.R.; Konduru, N.R. High accuracy resolver to digital converter based on modified angle tracking observer method. *Sens. Transducers* **2012**, *144*, 101–112.

22. Zhang, J.; Wu, Z. Automatic calibration of resolver signals via state observers. *Meas. Sci. Technol.* **2014**, *25*, 2223–2237. [CrossRef]

23. Wu, Z.; Li, Y. High-accuracy automatic calibration of resolver signals via two-step gradient estimators. *IEEE Sens. J.* **2018**, *18*, 2883–2891. [CrossRef]

24. Shi, T.; Hao, Y.; Jiang, G.; Wang, Z.; Xia, C. A method of resolver-to-digital conversion based on square wave excitation. *IEEE Trans. Ind. Electron.* **2018**, *65*, 7211–7219. [CrossRef]

25. Farid, T. Effect of damper winding on accuracy of wound-rotor resolver under static-, dynamic-, and mixed-eccentricities. *IET Power Electron.* **2018**, *12*, 845–851.

26. Saneie, H.; Alipour-Sarabi, R.; Nasiri-Gheidari, Z.; Tootoonchian, F. Challenges of finite element analysis of resolvers. *IEEE Trans. Energy Convers.* **2019**, *34*, 973–983. [CrossRef]

27. Pecly, L.; Schindeler, R.; Cleveland, D.; Hashtrudi-Zaad, K. High-precision resolver-to-velocity converter. *IEEE Trans. Instrum. Meas.* **2017**, *66*, 2917–2928. [CrossRef]

28. Ge, X.; Zhu, Z.Q.; Ren, R.; Chen, J.T. Analysis of windings in variable reluctance resolver. *IEEE Trans. Magn.* **2015**, *51*, 8104810. [CrossRef]